Article

Not peer-reviewed version

Carcinogenic Effect of Human Tumors-Derived Cell Free-Filtrates in Nude Mice

Jorge Berlanga-Acosta *, Ernesto Arteaga-Hernandez, Ariana Garcia-Ojalvo, Marisol Rodriguez-Touseiro, Dayanis Duvergel-Calderin, Jose Suarez-Alba, Dasha Fuentes-Morales, Osmany Mendoza-Fuentes, Laura Lopez-Marín, Gerardo Guillen-Nieto

Posted Date: 7 November 2023

doi: 10.20944/preprints202311.0357.v1

Keywords: Cells-free filtrate; tumor homogenate; cancer; nude mice; malignant transformation

Article

Carcinogenic Effect of Human Tumors-Derived Cell Free-Filtrates in Nude Mice

Jorge Berlanga-Acosta [1,*], Ernesto Arteaga-Hernandez [2], Ariana Garcia-Ojalvo [1], Dayanis Duvergel-Calderin [2], Marisol Rodriguez-Touseiro [2], Laura Lopez-Marín [3], José Suarez-Alba [1], Dasha Fuentes-Morales [4], Osmany Mendoza-Fuentes [1] and Gerardo Guillen-Nieto [1]

[1] Center for Genetic Engineering and Biotechnology, Biomedical Research Direction, Ave 31 SN e/158 and 190, Cubanacan, Playa 10600, Havana, Cuba
[2] Department of Pathology, Hermanos Ameijeiras Hospital, Calle San Lazaro #701, Centro Habana, La Habana 10400, Cuba
[3] Department of Pathology, Institute for Arteriosclerosis Research, Institute of Nephrology "Dr. Abelardo Buch", Calle 26 y Línea del Ferrocarril, Vedado, Havana 10400, Cuba
[4] National Center for Laboratory Animal Breeding, Calle 3ra, No 40759, Entre 6ta y Carretera de Tirabeque, Reparto La Unión, Boyeros, La Habana, Cuba
* Correspondence: jorge.berlanga@cigb.edu.cu

Abstract: Cancer remains as a worldwide cause of death. Investigational research efforts have included the administration of tumors-derived extracts to healthy animals. Having previously demonstrated that administration of non-transmissible, human cancers-derived homogenates induced malignant tumors in mice; we examined here the consequences of administering 50 or 100 μg of protein of crude homogenates from samples of mammary carcinoma, pancreatic adenocarcinoma, and melanoma. The protocol conceived six inoculations per week during three months. Concurrent control group received homogenates of healthy donor skin cosmetic surgery fragments. Mammary carcinoma homogenate administration did not provoke animals' deterioration or mortality. Multiple foci of lung adenocarcinomas with broad expression of malignity histomarkers, coexisting with small cell-like carcinomas were found. Disseminated cells, positive to classic epithelial markers were detected in lymphoid nodes. Pancreas tumor and melanoma homogenates administrations severely deteriorated animals' health. Pancreas tumor induced lung poorly-differentiated adenocarcinomas, as a remarkable pancreatic islets hyperplasia. Melanoma affected lungs with atypical adenomatous hyperplasia and solid pseudopapillary adenocarcinoma. Giant atypical hepatocytes with variegated nuclei were also observed. Kidney parenchyma exhibited dispersed foci of neoplastic cells within a desmoplastic matrix. A noticeable nuclear overlapping with hyperchromatic nuclei, mitotic figures, and prominent nuclear atypia was identified in epidermal cells. None of these changes were ever detected in any mouse of the control groups. This study confirms and extends our hypothesis that tumor homogenates contain and may act as a vector for "malignancy drivers", which ultimately implement a carcinogenesis process in otherwise healthy mice.

Keywords: cells-free filtrate; tumor homogenate; cancer; nude mice; malignant transformation

1. Introduction

The molecular drivers and pathways behind the multifaceted episode of cellular malignant transformation up to clinical cancer have remained elusive for years [1,2]. Thus, although no other human pathology has been so extensively and comprehensively investigated, there is still a long way to go in portraying the extensive horizon of cancer mysteries. Regardless of the large repertoire of innovative therapies available, this heterogeneous group of diseases still stands as a major cause of mortality worldwide [3].

Carcinogenesis is a vast process that stems from genetic and epigenetic alterations, including loss and gain-of-function mutations that occur in one single cell [4,5]. This seems to be a sequence of cumulative changes from initiation, promotion, progression [6,7]; and that translate in an expanding

 doi:10.20944/preprints202311.0357.v1

disorder in cellular organization under a microenvironmental pressure for survival [6]. Consequently, transformed cells are gifted with exclusive and distinctive capabilities including epigenetic plasticity, cytoprotective abilities, metabolic reprogramming, proliferative dynamism, dissemination skills, phenotypic transition, dormancy, and even local cannibalism [8–12].

The immortal and autonomous malignant cells also "educate" host immune system with lessons of tolerance, and ironically, use [8,13] inflammation for their own benefit [14–16] which contributes to the process of metastatic seeding in the new substrate [17,18]. Importantly, cancer cells are genuine "industries" of secreting soluble messages, being able to produce and deliver a broad variety of encapsulated or free signalers with multiple pathological implications [19,20]. After Bernard Peyrilhe inaugurated the investigative use of human cancer-derived fluids, the administration of filtered cell-free tumor homogenates to animals, has translated in groundbreaking contributions in experimental pathology [21]. We recently undertook the use of cells-free filtrates (CFFs) derived from fresh human pathologic tissue samples, to examine the hypothesis that the "chemical codes" of non-communicable diseases are imprinted in target tissues, that could be extracted, passively transferred to healthy animals, and accordingly reproduce the histological hallmarks of the human donor [22]. These experiments demonstrated that CFFs acted as a vehicle for delivering the soluble signalers that imposed the pathologic donors' phenotypes in otherwise normal animals [23,24]. Subsequently and following the hypothesis that CFFs may contain cell-transforming messengers, we examined the consequences on nude mice of administering the homogenates of surgically excised malignant tumors. Tumors-derived crude material induced premalignant and malignant changes in different organs, and in a narrow temporary window [25].

Here we describe the findings of three independent and extemporaneous experiments consistent on: (1) the reproducibility of lung adenocarcinomas following the administration of CFF derived from mammary ductal carcinomas, and (2) the induction of pre-neoplastic changes, and truthful malignancies resulting from the administration of pancreatic adenocarcinoma and a metastatic melanoma in otherwise normal nude mice.

2. Materials and Methods

2.1. Ethics and consents

The experimental protocols and the use of human tissues were reviewed and approved by the ethic committees of the National Center for Laboratory Animal Breeding, the Center for Genetic Engineering and Biotechnology, and Hermanos Ameijeiras Hospital (Havana, Cuba). Subjects provided written informed consent for the investigational use of their surgically excised material. These included healthy tissue (dermis and epidermis) serving for control groups derived from healthy female donors undergoing abdominal and facial cosmetic surgery. Malignant samples used in the study consisted of: (1) - Three triple negative mammary invasive ductal carcinomas (IDC) which resulted in high histological grade and intense mitotic index, with lymphatic/vascular permeation, and confirmed invasion of sentinel lymph nodes. Donors were female subjects ranging 34 to 46 years old, and white. (2)- A histologically well-differentiated pancreatic ductal adenocarcinoma from a 56 years old, white male subject. (3)-A metastatic melanoma to a cervical lymphatic ganglion obtained from a 32 years old black female patient. All the samples were collected during the surgical intervention, washed with ice-cold sterile normal saline to remove fibrin and debris, and cryopreserved in liquid nitrogen until processing for the CFFs preparation. Tumor samples fragments were as per protocol 10% buffered formalin fixed and paraffin processed for histological analysis. The oncologic samples were ultimately processed and used for the experiments having received pathologists' report of malignancy.

2.2. Preparation of cells free-filtrates (CFFs)

Collected tissue was allowed to thaw, weighed and approximately 100 mg of wet tissue were placed in 2 mL vial containing 1 mL of normal saline, homogenized using a Tissue Lyser II for 3 minutes at 30 revolutions per second. Samples were then centrifuged at 10 000 rpm for 10 minutes at

 doi:10.20944/preprints202311.0357.v1

4°C, sterilized by filtration through 0.2 µm nitrocellulose filters (Sartorius Lab Instruments), aliquoted into sterile Eppendorf vials and stored at -70°C. Given the histological similitude of the IDC samples, the three tumor samples were pooled to ensure larger material availability. For the three study protocols described here, protein concentration was used as the arbitrary unit of measurement to prepare and administer the inoculums.

2.3. CFFs biochemical characterization

All the biochemical parameters were determined by spectrophotometric methods using commercial kits. Pro-inflammatory markers included C reactive protein (CRP) [C Reactive Protein (PTX1) Human ELISA Kit, Abcam, Cambridge, UK]; interleukin (IL)-1β (IL-1 beta Human ELISA Kit, Abcam. Mass, USA); IL-6 (IL-6 Human ELISA Kit, Abcam); and tumor necrosis factor α (TNFα) (TNF alpha Human ELISA Kit, Abcam). Oxidative stress markers included malondialdehyde (MDA) [Lipid Peroxidation (MDA) Assay Kit, Abcam] and H_2O_2 (Hydrogen Peroxide Assay Kit, Abcam). Additionally, Situin 1 levels were determined using the ELISA Kit for Sirtuin 1 (SIRT1) (Cloud-Clone Corp., Houston, Texas, USA). In all cases, manufacturer's instructions were followed.

2.4. Animals

The three protocols described here were conducted with male BALB/c-Foxn1nu/Cenp mice (body weight 19-22 g) and age of 12 to 14, obtained from the National Center for Laboratory Animal Breeding (CENPALAB, Havana, Cuba) and maintained in ventilated racks (Tecniplast, Varese, Italy) in certified rooms for nude mice. Autoclaved food EAO 1004 (CENPALAB, Havana, Cuba) and water were offered ad libitum. Room temperature (20-23°C), humidity (65±10%) and the photoperiod cycles (12 h per day), were automatically controlled. The animals were observed twice a day by an experienced staff for health status. Body weight was registered a day before the study commencement, on a weekly basis and before autopsy. All procedures were performed according to local and International Guiding Principles for Biomedical Research Involving Animals. All animal studies were conducted under a protocol approved by the Institutional Animal Care and Use Committee from the National Center for Laboratory Animal Breeding (CENPALAB), and the Center for Genetic Engineering and Biotechnology, all in Havana, Cuba.

2.5. Administration protocols

Three study protocols corresponding to each tumor histotype CFF were settled: Examination of the effect of (I) Breast tumors, (II) Pancreatic ductal adenocarcinoma, and (III) Metastatic melanoma. For each protocol 24 BALB/c-Foxn1nu/Cenp mice were randomly distributed among two experimental arms (N=8/arm) receiving: (1) CFF derived from malignant tissue samples, (2) Control CFF derived from healthy donor skin. Mice in protocol I received 100µg of protein (as arbitrary unit) of normal skin tissue or breast malignant samples, whereas for protocols II and III protein concentration was reduced to 50µg – all in a volume of 250µL of normal saline, once a day, from Monday through Saturday for 12 weeks. We assumed this administration time window for the three protocols since it proved to induce malignant tissue changes in a previous study [25]. Subcutaneous and intraperitoneal routes were alternatively used on weekly bases to prevent local injury due to repeated trauma.

2.6. Autopsy, tissue processing, and immunohistochemistry

Animals were euthanized under terminal anesthesia at the end of the administration period. Alternatively, mice that along the administration period evolved to an extreme clinical condition were sacrificed to ensure a proper autopsy and organs collection (as described below). Autopsy study was conducted following an internal protocol based on described techniques [26]. Gross noticeable changes in organs and tissues were recorded, and fragments collected for histopathological analysis. Representative fragments from apparently normal organs were also harvested. Samples were 10% buffered formalin fixed, paraffin-embedded, and serial 5-µm sections stained using H&E. Images

 doi:10.20944/preprints202311.0357.v1

were captured using a BX53 Olympus microscope, coupled to a digital camera and central command unit (Olympus Dp-21). Histological examinations were blindly performed by two MD pathologists, experienced in experimental pathology (EAH, DDC, and LLM). Histopathological findings of premalignant and malignant lesions were collectively discussed, and ultimately diagnosed in accordance to current recommendations [27,28]. Paraffin sections of representative tissue lesions in mice receiving the tumors material and corresponding specimens from control counterparts, were mounted on poly-l-lysine coated slides (DAKO, California, USA) in order to reduce inter-tissue/experimental variations along immunohistochemistry studies. The slides were dewaxed and rehydrated through graded washes of ethanol. Rehydrated slides were exposed to high pH antigen retrieval solution (DAKO, USA) for 20 minutes at 90°C. Following equilibration at room temperature, slides were washed in PBS and endogenous peroxidase blocked. Unspecific binding blocking solution was used for 20 min and the sections incubated for other 40 minutes with antibodies directed to: TTF-1 (Santa Cruz Biotechnology Sc53136. 1/100), c-Myc (Abcam, ab32072. 1/100), PCNA (Cell Signaling Technology (PC10) Mouse mAb #2586. 1/250), estrogen receptor (Santa Cruz Biotechnology (D-12): SC-8005, 1/250), progesterone receptor (Santa Cruz Biotechnology, FKBP51 SC-271547, 1/250), HER-2 (Santa Cruz Biotechnology, ErbB2/HER2 (A-2): SC-393712, 1/200), TERT, telomerase reverse transcriptase (Abcam, ab216625, 1/150), Survivin (Abcam, ab469, 1/200), CD56 (Invitrogen Cat #PA5-78402, 1/200), CD45 antigen (leukocyte common antigen, Abcam, ab10558, 1/100), and cytokeratin 7, CK7 (Abcam, ab181598, 1/250). Antigen retrieval was conducted according to each antibody manufacturer instructions protocol. The immunolabeling reaction was developed as described for the Mouse and Rabbit Specific HRP/DAB (ABC) Detection IHC kit (Abcam, ab64264). Non-specific tissue labelling internal controls included the omission/replacement of the primary antibody by the background reducing antibody diluent, and normal rabbit serum (Boster Biological Technology, Pleasanton CA, USA, catalog # AR1010).

2.7. Statistical processing

Statistical analyses were performed using GraphPad Prism 6.01 software. Normal distribution was analyzed using D'Agostino-Pearson and Shapiro-Wilk normality tests. Variance homogeneity was evaluated using Brown-Forsythe and Bartlett's tests. Comparisons between groups along the study were carried out using two-way ANOVA followed by Sidak's multiple comparisons test. Survival data were analyzed using the Log-rank Mantel-Cox test. Values of $p<0.05$ indicated statistically significant differences.

3. Results

3.1. I-Cells-free filtrates descriptive biochemical characterization

As described, surgical pieces of healthy donors' skin and fragments of three different human malignant tumors were used to prepare the CFFs. The elemental biochemical description shown in Table 1 indicates that cellular lipids undergoing a peroxidation process is similar among the healthy skin, and the tumor samples as reflected by the MDA levels. However, metastatic melanoma seems to have an important generation of superoxide anion and hydroxyl radicals as judged by the H_2O_2 levels, which exceeded between 4 and 6 folds the values determined for the healthy control skin and the other malignant samples. Tumors-derived samples seemed to exhibit a particular inflammatory signature. CRP appeared particularly elevated in pancreatic adenocarcinoma exceeding over 24 folds the concentration detected in metastatic melanoma, and healthy control skin. Melanoma-derived CFF however, showed the highest level of IL-6, followed by pancreatic adenocarcinoma. In line with this, melanoma also exhibited the largest concentration of IL-1β, TNFα, and Sirtuin-1 which was followed by the concentration determined in mammary carcinoma homogenate. Of note, healthy donor skin tissue homogenate showed the lowest values of IL-1β whereas IL-6, TNFα, and Sirtuin-1 were not detected (Table 1).

Preprints (www.preprints.org) | NOT PEER-REVIEWED | Posted: 7 November 2023 doi:10.20944/preprints202311.0357.v1

Table 1. Biochemical characterization of the CFFs.

Samples	MDA (μM)	H_2O_2 (pmol/μL)	CRP (ng/mL)	IL-6 (pg/mL)	IL-1β (pg/mL)	TNFα (pg/mL)	Sirtuin 1 (ng/mL)
Control healthy donor skin	3.47	17.39	21.95	ND	25.80	ND	ND
Mammary ductal carcinoma	3.89	25.88	152.39	30.15	116.18	72.89	17.21
Pancreatic ductal adenocarcinoma	3.05	21.66	529.75	151.39	99.70	27.25	5.30
Metastatic Melanoma	4.20	108.43	18.35	262.40	807.24	127.18	23.01

ND: not detectable.

3.2. I-Protocol 1. Breast tumors CFF administration

Mammary carcinoma CFF administration was not associated to behavioral changes, clinical deterioration, or somatic emaciation. Body weight remained similar between the mice groups treated with malignant and healthy tissue homogenates until the day of autopsy (20.17 ± 1.73-vs-21.23 ± 118, p=0.96). As there was no mortality during the 3 months period, all the animals were terminated and autopsied as scheduled.

Administration of breast carcinomas homogenate for 12 weeks generated premalignant and malignant changes in lung tissue. Lungs microscopic examination in all these mice (N=8), exhibited extensive areas of parenchymal condensation in which atypical adenomatous hyperplasia (AAH) at the expenses of type 2 pneumocytes with clear, enlarged, and atypic nuclei predominated (not shown). In these areas of parenchymal condensation and alveolar luminal encroachment, large subpleural nodules diagnosed as adenocarcinoma of both solid and lepidic growth were distinguished (Figure 1A). Mice treated with the healthy skin homogenate showed a morphologically normal pulmonary parenchyma (Figure 1B). The immunohistochemical characterization of these nodules confirmed their authentic malignant nature. Tumors cells exhibited a strong nuclear signal for TTF-1 (Figure 1C) which contrasted with the controls' specimens restricted expression (Figure 1D). These cells also exhibited a remarkable cytoplasmic HER-2 expression (Figure 1E) as compared to controls (Figure 1F). Broad nuclear expression of PCNA, was observed in the tumor-bearing mice (Figure 1G), as compared to the expression in lungs normal parenchyma of healthy skin-treated mice (Figure 1H). Nuclear and cytoplasmic c-*Myc* overexpression that extended to areas of microscopically normal alveolar walls was found in the lungs of breast-tumors inoculated mice (Figure 1I). Control mice alveolar walls however, exhibited only a marginal immunolabeling (Figure 1J). Meaningfully nuclear TERT expression was observed in these tumors, concurrent to overexpression of nuclear survivin, nuclear estrogen, and progesterone receptors as part of the tumors' phenotype (not shown). Within these tumors, conglomerates of cells appeared organized forming rosette-like structures that encircled arterioles and bronchioles. The rosette-like aggregates were heterogeneous and contained large, atypical, irregular epithelial, CK7 positive cells (not shown); and small, round, blue cells, that often appeared with large-sized vesiculous nuclei with lax chromatin, and central conspicuous nucleoli. Immunohistochemistry demonstrated that of these cells were negative to CD45 (not shown) whereas some cells were found positive to CD56, suggesting its neuroendocrine origin (Figure 1K). These round blue cells were often visualized forming subpleural, periarteriolar, and peribronchial nodules with notorious nuclear molding, presumptively identified as small cell lung carcinoma (Figure 1L). Finally, an interesting immunohistochemical finding was the presence of HER-2, CK7, estrogen, and progesterone receptors positive cells, in the subcapsular

 doi:10.20944/preprints202311.0357.v1

sinus of thoracic lymphoid nodes. Intense nuclear labeling for both hormones receptors was observed in these cells. Figure 1M demonstrates the intense expression of progesterone receptor; in as much, lymphatic node samples from the mice control group were negative to HER-2, and CK7. A faint staining for progesterone (Figure 1N) and estrogen receptors appeared circumscribed to cell membrane.

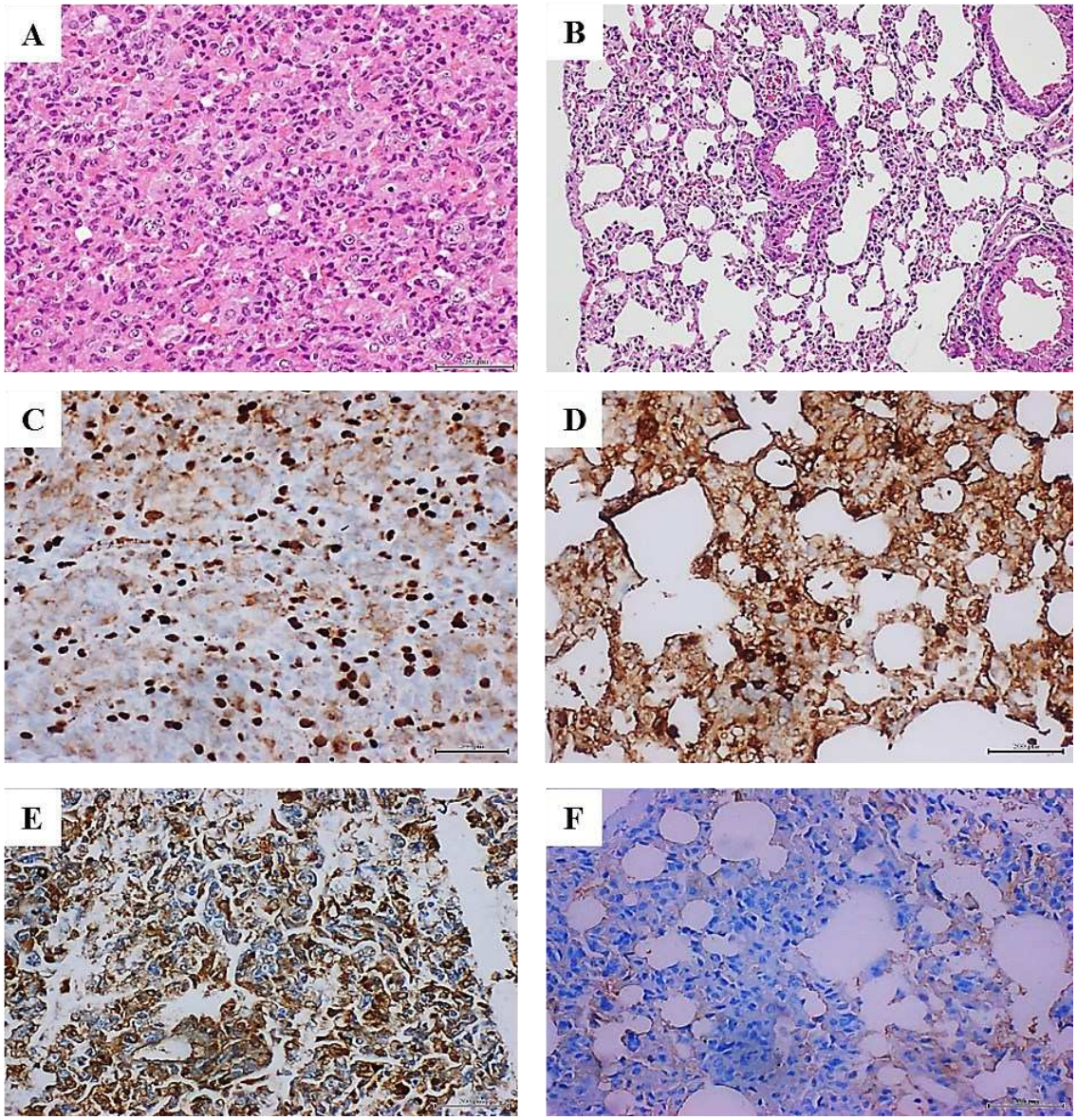

Preprints (www.preprints.org) | NOT PEER-REVIEWED | Posted: 7 November 2023 doi:10.20944/preprints202311.0357.v1

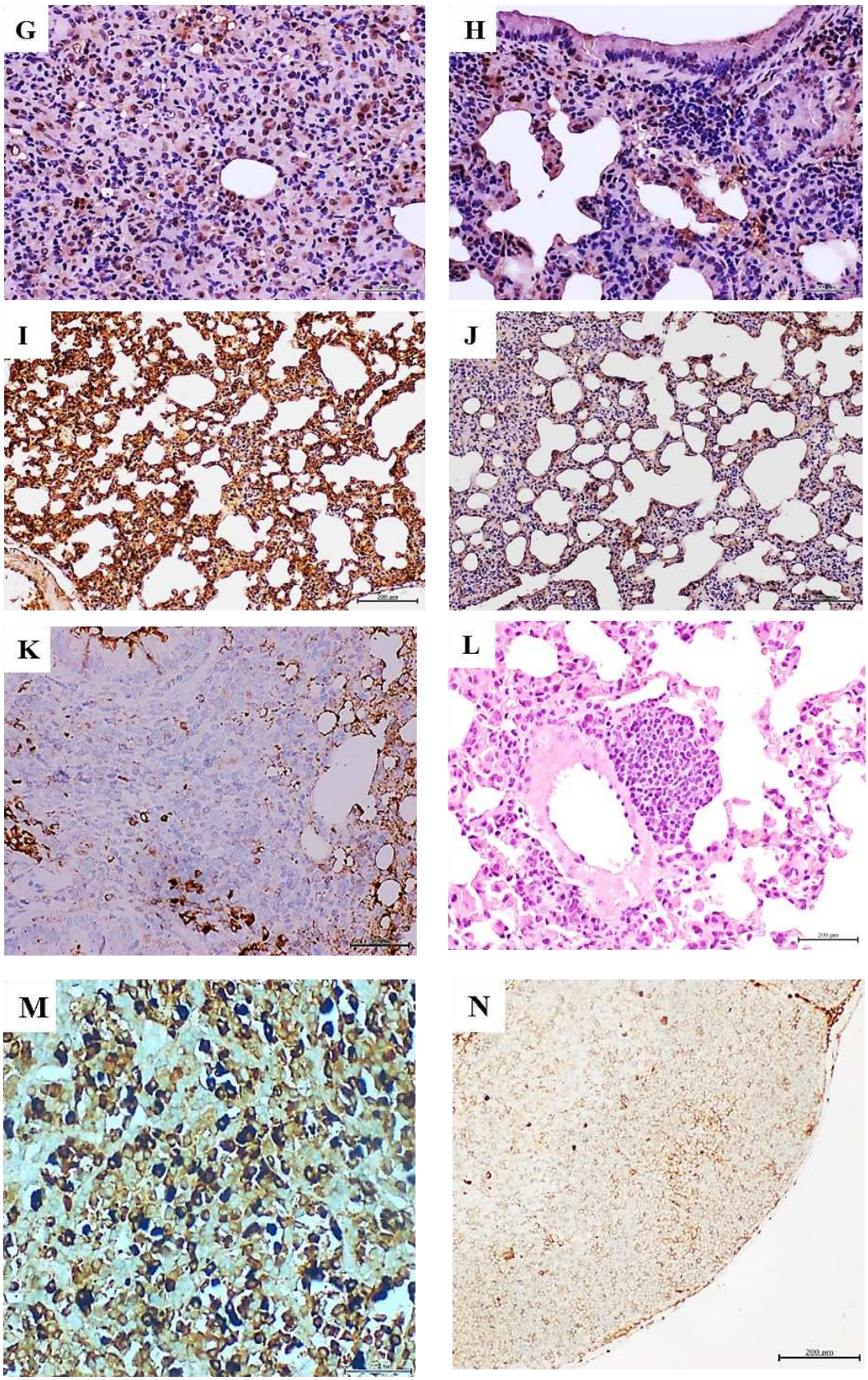

Figure 1. Histopathological and immunohistochemical characterization of lung tumors in mammary carcinoma-treated mice. A: Histological image representative of the solid growth pattern of a lung adenocarcinoma in animals treated with the homogenate of triple negative breast tumor. The intense cellular proliferation erased the alveolar lumen, in sharp contrast with the normal aspect of lungs

 doi:10.20944/preprints202311.0357.v1

parenchyma in animals from the control group as shown in B. H/E x 40. C: An intense and broadly distributed nuclear immunohistochemical expression of TTF-1 observed in the lung adenocarcinomas of the mammary tumor-treated mice group. D shows that few stained TTF-1 positive nuclei are counted in the alveolar walls of the control group x40. Tumor-treated mice lung samples were positive to HER-2 expression, basically in the cytoplasm and cell membrane –in E, whereas this marker was not expressed by lung cells of mice from the control group F, x40. Large and intense nuclear immunolabeling was found for the cell proliferation marker PCNA by the tumor cells as shown in G. Lung cells from the control group exhibited a far more restricted expression to alveolar walls-H, x20. As it is illustrated in I, there is a broad and intense oncogene c-Myc expression even by normal alveolar walls adjacent to the adenocarcinoma nodules. Conversely, lungs from control mice -J- showed a faint and marginal immunolabeling x20. K demonstrates that within the periarteriolar and peribronchiolar rosette-like conglomerates, some atypical round, small, blue cells were positive to CD56 signal, indicating a neuroendocrine line, x40. The presence of a nodule made up by round, blue cells suggestive of a small cell carcinoma is shown –L, attached to the adventitia of a large vessel, H/E x 20. Mediastinal lymphatic nodes from mice treated with the breast tumor, exhibited cells immunoreactive to cytokeratin 7, HER-2, and hormone receptors. Here an intense and specific nuclear signal for progesterone receptor is illustrated in M. This reaction is contrasting with the negligible immunolabeling shown by the node lymphatic cells- shown in N -from control mice receiving normal skin homogenate. There is also appreciable difference in nuclear size between both samples. 5-μm sections. Magnification x40 for both. Scale bar is 200 μm for all.

3.3. Protocol 2. Pancreatic ductal adenocarcinoma CFF administration

Having elapsed 6 injections of the tumor CFF, animals began to show asthenia, tendency to isolation, hunched posture, and frail, dry, and flaky skin. Although at the second week the dose was deescalated to 50 μg in order to prevent animals' decay, the aspect of "ill condition" continued with evident emaciation from the second month onward (20.14±0.85 vs 23.25±2.02, p=0.04). Four animals with progressive clinical and somatic deterioration were untimely terminated and autopsied, whereas the other four mice although in a consumptive state completed the administration phase (autopsy weights: 18.43±1.54 vs 22.86±1.12, p=0.02). Healthy donor's skin-treated mice remained active and healthy during all the administration period. The eight animals were autopsied as per protocol scheduled.

The histopathologic examination of mice organs' exposed to pancreatic tumor CFF revealed that again, the lungs appeared to be the major target structure with pre and malignant changes. Two major findings were obtained: multiple foci of solid, poorly differentiated adenocarcinoma across the lung parenchyma (Figure 2A), and a marked hyperplasia of pancreatic Langerhans islets (Figure 2B). Alveolar/bronchiolar hyperplasia and atypical adenomatous hyperplasia (AAH) were the only findings attributable to the pancreatic tumor CFF in mice prematurely autopsied. Nevertheless, immunohistochemistry revealed a strong nuclear and cytoplasmic TTF-1 expression by the bronchoalveolar cells within these foci of AAH (not shown). None of the mice treated with the healthy donor's skin homogenate exhibited microscopic pathologic changes; including the normal aspect of Langerhans islets (Figure 2C).

Preprints (www.preprints.org) | NOT PEER-REVIEWED | Posted: 7 November 2023 doi:10.20944/preprints202311.0357.v1

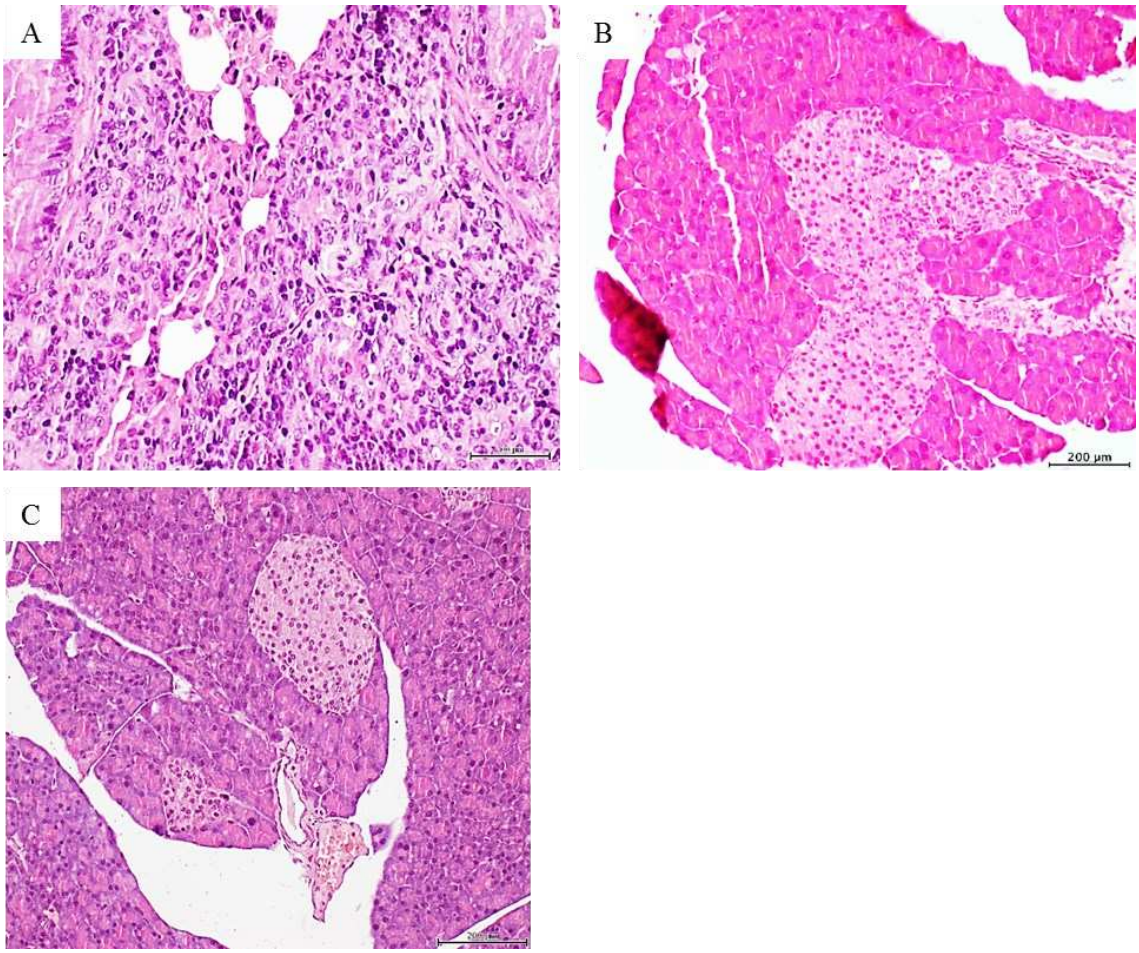

Figure 2. Histopathological changes detected in mice treated with the pancreas adenocarcinoma. A: Histological panoramic image representative of the poorly-differentiated, solid adenocarcinomas found in mice treated with the pancreas adenocarcinoma homogenate. There is an obvious matrix disorganization, cellular overcrowding, nuclear pleomorphism and atypia. H/E x 20. The pancreas tumor homogenate also impacted on the mice pancreas given by a remarkable Langerhans islets hypertrophy as shown in B. Pancreas from those mice treated with the healthy skin homogenate exhibited a normal aspect on the islets and the pancreas in general (C). 5-µm sections. H/E staining. Magnification x 10. Scale bar 200 µm for all.

3.4. Protocol 3. Metastatic melanoma CFF administration

The administration of 50 µg of melanoma-derived protein also led to a consumptive process and clinical involution in 6 animals. Consequently, mice were untimely and gradually autopsied on days 34, 36, 43, 45, 49 and 55 due to their deteriorated condition. On day 61 the only two remaining mice were autopsied and the study concluded. Mice treated with the healthy donor's skin remained normal and active during the two-month administration period. Two mice of this group were found dead on days 57 and 60 with evidences of autolysis.

Melanoma-derived CFF induced pre-malignant and malignant proliferative changes that involved lungs, liver, kidneys, and skin. Bronchoalveolar proliferative changes extended from AAH to intra-alveolar pseudo-papillary adenocarcinomas, which were made up by round blue cells, with atypical and overlapping irregular nuclei, exhibiting hyperchromasia and clumped chromatin. Another cell population observed in this conglomerate showed large vesiculous nuclei, with coarse dispersed chromatin, and prominent nucleoli (Figure 3A). In line with this pathologic proliferation in the lungs, is the identification of circulating tumor cells as an embolus within a lymphatic vessel lumen, integrated by a cluster of cells with the same cytological traits as described above (Figure 3B). In relation to liver, two major alterations were identified: (1) presence of nodules or aggregates of

Preprints (www.preprints.org) | NOT PEER-REVIEWED | Posted: 7 November 2023 doi:10.20944/preprints202311.0357.v1

cells of putative leukocytic origin with small, irregular and atypical nuclei, scattered across the liver parenchyma (not shown), and (2) the presence of voluminous hepatocytes with large, atypical, variegated nuclei containing coarsely granular or disperse chromatin (Figure 3C). A liver normal histology was observed in the group of control mice (Figure 3D). In kidneys parenchyma, infiltration of neoplastic cells was found in the interstitium, peritubular capillaries and in the lumen of the tubules, demonstrating cellular atypia, irregular nuclei, pleomorphism and prominent nucleoli. There is also an interstitial inflammatory infiltrate of lymphocytes and polymorphonuclear neutrophils with a desmoplastic reaction (Figure 3E). By the contrary, animals from the control group showed no pathological changes in kidneys parenchyma (Figure 3F). Skin from melanoma treated mice also revealed an abnormal and irregular epidermal proliferative disorder, which included epidermis and the epithelial dermal ridges. Epidermal cells were seen with noticeable nuclear overlapping, the presence of irregular, sharply angulated and hyperchromatic nuclei, mitotic figures, and prominent nuclear atypia (Figure 3G). Control mice-skin showed no histopathological alterations (Figure 3H).

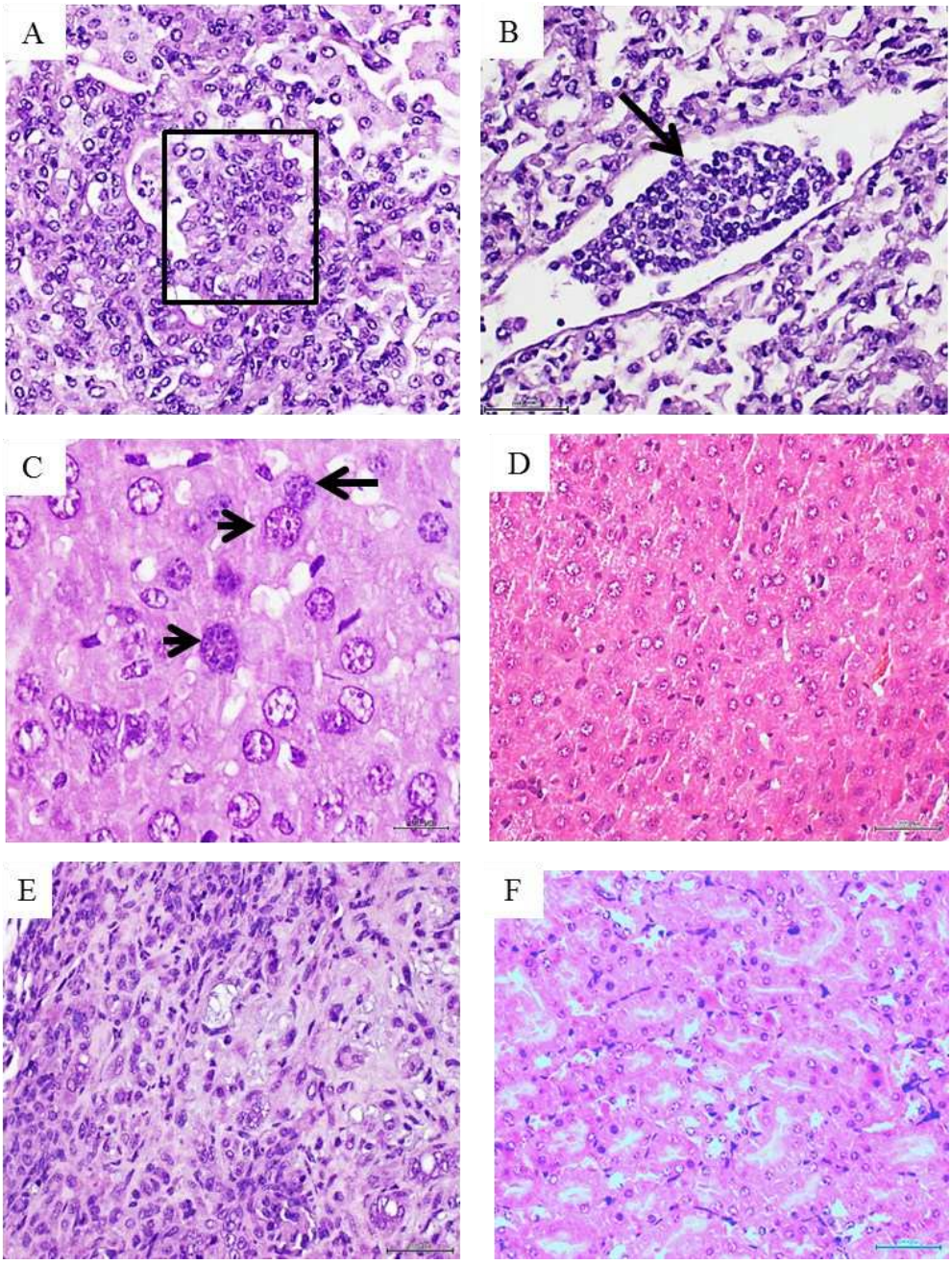

 doi:10.20944/preprints202311.0357.v1

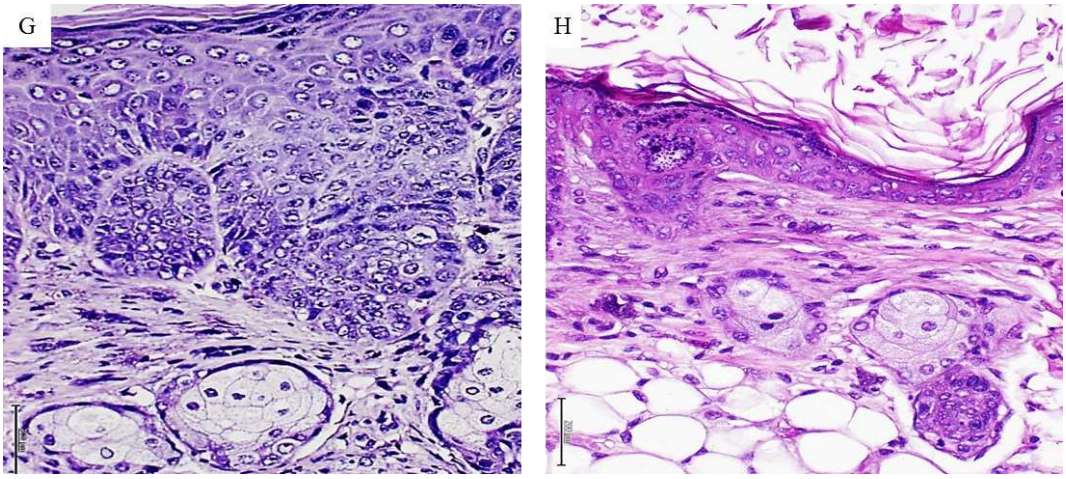

Figure 3. Histopathological changes detected in mice treated with metastatic melanoma. A: Histological image representative of a solid adenocarcinoma with pseudopapillary growth pattern in a mouse treated with the metastatic melanoma homogenate. The papillae within the box show the overlapping of atypical nuclei. Correspondingly, a conglomerate of heterogeneous cells with scant cytoplasm and occupying the lumen of a lymphatic vessel is shown in image B (black arrow). The cells are morphologically similar to those observed in tumor nodules and papillae, suggesting the migration/circulation of tumors-derived cells. Both H/E x 20. Melanoma CFF induced enlargement in hepatic cells and their nuclei. As shown in C, enlarged, atypical, variegated nuclei with coarse chromatin were found across the liver parenchyma (black arrow). A normal aspect of the liver parenchyma derived from normal skin-treated mice appears in image D. Both H/E x 40. Infiltration of neoplastic cells in kidneys from melanoma-treated mice -E-, involved the interstitium, peritubular capillaries, and the tubular lumen. An interstitial inflammatory infiltrate with a desmoplastic reaction is noticeable. This image of matrix disorganization and cellular pleomorphism is fully divergent with the aspect of normal kidney parenchyma from control mice as seen in F. Both H/E x 20. G: An aberrant and irregular proliferation of epidermal cells with prominent nuclear atypia, overcrowding, and mitotic figures was induced by the melanoma homogenate. There is an evident difference with the epidermal layer cellularity and organization corresponding to control group mice as depicted in H. Both H/E x 20. 5-µm sections and scale bar 200 µm for all.

4. Discussion

To experimentally examine the hypothetical existence of a soluble and transferable tumor tissue drivers, crude homogenates from human tumors were inoculated in nude mice: triple negative-invasive ductal mammary carcinoma, pancreatic ductal adenocarcinoma, and a metastatic melanoma are three varieties of poor prognosis cancers, with limited treatment options, ability to develop resistance to therapies, and with dismal 5-year survival rates [29–32].

Irrespective to its limitations, this study confirms, extends, and consequently supports our hypothesis that human malignant tissues-derived homogenates are able to disrupt the proliferative and differentiation programs of normal host cells, conducting to the onset of premalignant and malignant changes. A previous study from our group addressing the effects of 3 months administration of an invasive mammary carcinoma, and a pleomorphic sarcoma-derived CFFs, proved to act as a genuine carcinogen in nude mice, rendering epithelial and mesenchymal tumors that exhibited irreversible, metastasizing, and autonomous progression [25]. The findings obtained in the present study while administering the breast carcinoma-derived CFF to mice, faithfully reproduce and converge with these previous pathologic descriptions [25]. We deem this is a meaningful event given that the multidimensional complexity of cancer has historically derived in variability, heterogeneity, and lack of reproducibility in basic research experiments [33].

The experimental methodology used in this opportunity was as previously described [25], so that tumors-derived CFFs were prepared using sterile physiologic saline solution with no purification processes, or any other type of chemical manipulation. These homogenates represent a

 doi:10.20944/preprints202311.0357.v1

pure extract of the pathologic tissues, a rich-in-content material, and a vehicle of donor cells' soluble signatures that have previously proved to recapitulate in healthy recipient rodents, histopathologic hallmarks of diabetic angiopathy and neuropathy, and non-diabetic related arteriosclerosis as models of non-communicable chronic diseases [23,24]. We observed that despite the mechanical processing of tissue disruption to elaborate the CFFs, molecules of DNA and RNA from tumors homogenates could be quantitated, and RNA successfully reverse-transcribed and its product amplified, turning conceivable the hypothesis of a possible uptake by host's normal cells of some sort of tumor-derived genetic or epigenetic transformation driver [25].

Given the fact that none of these alterations were identified in any of the control animals, suggests that there was no spontaneous tumorigenesis during the experimental period, and that the neoplastic traits observed, do not represent a form of tissue reactive response to the human xenogeneic material. This later contention is supported by the following observations: (1) tumors-homogenates pathologic consequences in animals involved a microscopically typical disorder of cellular proliferation and differentiation. (2) The transformed tissues adopted an abnormal immunohistochemical profile, typical of legitimate malignancies. (3) The absence of a reactive, immuno-inflammatory response associated to human material inoculation or the tumor itself.

The simple and descriptive biochemical characterization of the three tumors and the healthy skin used as control; indicated that tumors, particularly metastatic melanoma exhibit elevated peroxidative and pro-inflammatory profiles. Melanoma-derived CFF presented the highest concentrations of H_2O_2 and IL-6, IL-1, TNF-α, and Sirtuin 1. These are all well-renown tumor biomarkers associated to carcinogenesis and malignant progression, cancer invasiveness, chemotherapy resistance, metastasis, and that in general correlate with worse prognosis [34–38]. Conversely, most of these biomarkers were not detected in control healthy skin-derived homogenate. It is likely that the pro-oxidative profile and the inflammatory signature of the tumors exerted a toxic imprinting in the recipient animals, which may explain the differences observed in the clinical evolution and the pathologic spectrum in each experimental protocol. This hypothesis is supported by the clinical reaction and the progressive mortality registered in mice receiving the melanoma, and secondly by those treated with the pancreatic adenocarcinoma; even when the initial dose was deescalated to prevent the collapse of the experiment. Furthermore, animals treated with melanoma CFF also showed a broader profile of proliferative changes encompassing lungs, liver, kidneys, and skin; whereas pancreas and breast tumors impact appeared circumscribed to lungs. Aside from the clinical toxicity exerted by the melanoma and the pancreas adenocarcinoma as compared to breast carcinoma effect, a common pathogenic outcome was the induction of *bona fide* lung adenocarcinomas, frequently classified as poorly differentiated. We had previously observed this type of lung tissue tropism in mice treated with breast carcinoma and pleomorphic anaplastic sarcoma CFFs [25]. The signalers and mechanisms behind this particular tissue tropism for lungs remain intriguing for us.

It is also difficult to explain why breast carcinoma-treated mice, having large areas of lung parenchymal condensation by tumoral growth, animals remained clinically normal and not emaciated. A simple interpretation of this observation is that these were "indolent-like tumors" and that one thing is to host a malignant tumor, and another one is to be sick by cancer. An interesting and unusual finding observed in 3 mice treated with the breast carcinoma, is the coexistence of two histologically different tumors within the same lung. On one side, solid and lepidic patterns adenocarcinomas overexpressing a set of well-validated malignancy immunohistochemical markers [39–41], and on the other side, small cells carcinomas made by the typical small, round, blue cells, positive to a neuroendocrine marker. This tumors co-existence is a rare event. Although mouse lung neuroendocrine tumors have been genetically modeled by combined knockouts of different tumor suppressor genes [42], studies indicate that small cells-neuroendocrine carcinomas, do not develop spontaneously in mice [43]. This observation may advise on the carcinogenic nature of the tumors-derived CFFs.

Another interesting finding in breast tumor-treated mice, is the presence of cells of putative epithelial origin and intensely expressing estrogen and progesterone receptors, CK7, and HER-2 in

the subcapsular sinuses of mediastinal lymphoid nodes. This fact incites to suggest that these lung adenocarcinoma conglomerates are already contributing to a pool of circulating cells, which may be disseminating and colonizing. Dissemination and colonization are pieces of the metastatic phenomenon which is considered a late event relative to tumor initiation [44,45].

In our previous [25] and in the present study, another unexplained observation relates to the short time window in which pre-malignant changes and malignant tumors are established, particularly viewed under the scope of the canonic multistage path of initiation-promotion-progression [46].

The fact that we have been unable so far to identify the tumor-derived signalers that may elicit the *in vivo* carcinogenic response, is a major limitation of this study. Nevertheless, it confirms that CFF is a vector of some "malignant code" contained within human non-transmissible tumor cells, which may implement a carcinogenesis process. This study is also the fourth in a line that concurs to support the hypothetical existence and transmissibility of a "pathologic cellular memory", encrypted in the "diseased cells", with no interspecies barrier, and that is able to impose the recapitulation of the human donor's pathologic traits. In addition to the potential therapeutic significance derived from the identification of these carcinogenesis primers, we deem that these studies offer an additional practical and useful platform for *in vivo* cancer modelling.

Supplementary Materials: Not applicable. There is no supplementary material.

Author Contributions: JBA. Original idea: study design, practical implementation, samples collection, interpretation and manuscript preparation. **EAH. Study design:** practical implementation, histopathologic analysis and interpretation. **AGO. Study design:** biochemical samples analysis, statistical analysis and interpretation. **DDC. Study design:** histopathologic analysis and interpretation. **M**RT. Practical implementation, immunohistochemical processing and interpretation. **LLM. Study design:** histopathologic analysis and interpretation. **JSA. Study design:** practical implementation, samples collection, and histological processing and image curation. **DFM. Study design:** practical implementation, samples collection data processing. **OMF. Study design:** practical implementation, animal care and management, samples collection.**GGN. Study design:** practical implementation, and general administrative support.

Funding: The funds used for this study were provided by BioCubaFarma Holding – addressed to CIGB/IBM/Cicatrización Account number 3051-280.

Institutional Review Board Statement: Herein we declare that the protocol for this study using nude mice were reviewed and approved by the ethic committees of the National Center for Laboratory Animal Breeding (animal provider center) and the Center for Genetic Engineering and Biotechnology (recipient center). Havana, Cuba.

Informed Consent Statement: We declare here that all the patients undergoing oncologic and cosmetic surgery, approved and issued informed consent for the investigational use of samples from their excised tissues.

Data Availability Statement: All the data related to this investigation has been included in the present manuscript. Authors will be happy to reply before any request, exchange invitation, or collaboration proposal from readers.

Acknowledgments: Authors express their gratitude to Dr. Indira Martinez-Jiménez and Dr. Nadia Rodríguez-Rodríguez for their valuable technical assistance in general samples collection and evolvement of melanoma-derived samples study. We also are indebted to Dr. Jorge Castro-Velazco for his organizational support in animals' health care.

Conflicts of Interest/Disclaimer: We declare no conflict of interest.

References

1. Bordonaro M. Quantum biology and human carcinogenesis. *Biosystems*. 2019;178: 16-24.
2. NCI. What Is Cancer? 2021 [cited 2023; National Cancer Institute]. Available from: https://www.cancer.gov/about-cancer/understanding/what-is-cancer
3. Siegel RL, Miller KD, Wagle NS, Jemal A. Cancer statistics, 2023. *CA Cancer J Clin*. 2023;73(1): 17-48.
4. Cataisson C, Lee AJ, Zhang AM, Mizes A, Korkmaz S, Carofino BL, Meyer TJ, Michalowski AM, Li L, Yuspa SH. RAS oncogene signal strength regulates matrisomal gene expression and tumorigenicity of mouse keratinocytes. *Carcinogenesis*. 2022;43(12): 1149-61.
5. Lai TY, Ko YC, Chen YL, Lin SF. The Way to Malignant Transformation: Can Epigenetic Alterations Be Used to Diagnose Early-Stage Head and Neck Cancer? *Biomedicines*. 2023;11(6).

6. Nijman SMB. Perturbation-Driven Entropy as a Source of Cancer Cell Heterogeneity. *Trends Cancer*. 2020;6(6): 454-61.
7. Sarwar MS, Ramirez CN, Dina Kuo HC, Chou P, Wu R, Sargsyan D, Yang Y, Shannar A, Mary Peter R, Yin R, Wang Y, Su X, Kong AN. The environmental carcinogen benzo[a]pyrene regulates epigenetic reprogramming and metabolic rewiring in a two-stage mouse skin carcinogenesis model. *Carcinogenesis*. 2023;44(5): 436-49.
8. Grunt TW, Heller G. A critical appraisal of the relative contribution of tissue architecture, genetics, epigenetics and cell metabolism to carcinogenesis. *Prog Biophys Mol Biol*. 2023;182: 26-33.
9. Kariagina A, Lunt SY, McCormick JJ. Genomic and metabolomic analysis of step-wise malignant transformation in human skin fibroblasts. *Carcinogenesis*. 2020;41(5): 656-65.
10. Missiroli S, Perrone M, Genovese I, Pinton P, Giorgi C. Cancer metabolism and mitochondria: Finding novel mechanisms to fight tumours. *EBioMedicine*. 2020;59: 102943.
11. Phan TG, Croucher PI. The dormant cancer cell life cycle. *Nat Rev Cancer*. 2020;20(7): 398-411.
12. Torres AJF, Duryea J, McDonald OG. Pancreatic cancer epigenetics: adaptive metabolism reprograms starving primary tumors for widespread metastatic outgrowth. *Cancer Metastasis Rev*. 2023;42(2): 389-407.
13. Hanahan D. Hallmarks of Cancer: New Dimensions. *Cancer Discov*. 2022;12(1): 31-46.
14. Abbott M, Ustoyev Y. Cancer and the Immune System: The History and Background of Immunotherapy. *Semin Oncol Nurs*. 2019;35(5): 150923.
15. Gonzalez H, Hagerling C, Werb Z. Roles of the immune system in cancer: from tumor initiation to metastatic progression. *Genes Dev*. 2018;32(19-20): 1267-84.
16. Kim SK, Cho SW. The Evasion Mechanisms of Cancer Immunity and Drug Intervention in the Tumor Microenvironment. *Front Pharmacol*. 2022;13: 868695.
17. Han Y, Wang D, Peng L, Huang T, He X, Wang J, Ou C. Single-cell sequencing: a promising approach for uncovering the mechanisms of tumor metastasis. *J Hematol Oncol*. 2022;15(1): 59.
18. Weiss F, Lauffenburger D, Friedl P. Towards targeting of shared mechanisms of cancer metastasis and therapy resistance. *Nat Rev Cancer*. 2022;22(3): 157-73.
19. Liu K, Dou R, Yang C, Di Z, Shi D, Zhang C, Song J, Fang Y, Huang S, Xiang Z, Zhang W, Wang S, Xiong B. Exosome-transmitted miR-29a induces colorectal cancer metastasis by destroying the vascular endothelial barrier. *Carcinogenesis*. 2023;44(4): 356-67.
20. Pardini B, Sabo AA, Birolo G, Calin GA. Noncoding RNAs in Extracellular Fluids as Cancer Biomarkers: The New Frontier of Liquid Biopsies. *Cancers (Basel)*. 2019;11(8).
21. Elemento O. The road from Rous sarcoma virus to precision medicine. *J Exp Med*. 2021;218(4).
22. Berlanga-Acosta J, Fernandez-Mayola M, Mendoza-Mari Y, Garcia-Ojalvo A, Martinez-Jimenez I, Rodriguez-Rodriguez N, Garcia Del Barco Herrera D, Guillen-Nieto G. Cell-Free Filtrates (CFF) as Vectors of a Transmissible Pathologic Tissue Memory Code: A Hypothetical and Narrative Review. *Int J Mol Sci*. 2022;23(19).
23. Berlanga-Acosta J, Fernandez-Mayola M, Mendoza-Mari Y, Garcia-Ojalvo A, Martinez-Jimenez I, Rodriguez-Rodriguez N, Playford RJ, Reyes-Acosta O, Lopez-Marin L, Guillen-Nieto G. Intralesional Infiltrations of Arteriosclerotic Tissue Cells-Free Filtrate Reproduce Vascular Pathology in Healthy Recipient Rats. *Int J Mol Sci*. 2022;23(3).
24. Berlanga-Acosta J, Fernandez-Mayola M, Mendoza-Mari Y, Garcia-Ojalvo A, Playford RJ, Guillen-Nieto G. Intralesional Infiltrations of Cell-Free Filtrates Derived from Human Diabetic Tissues Delay the Healing Process and Recreate Diabetes Histopathological Changes in Healthy Rats. *Front Clin Diabetes Healthc*. 2021;2: 617741.
25. Berlanga-Acosta J, Mendoza-Mari Y, I M-J, Suarez-Alba J, Rodríguez-Rodríguez N, García Ojalvo A, Fernández Mayola M, rosales p, E A, Duvergel-Calderin D, I B, Campal-Espinosa A, Morales D, Vázquez E, Zamora-Sanchez J, Je M-S, Toro E-D, Gomez-Cabrera E, Guillen G. Induction of Premalignant and Malignant Changes in Nude Mice by Human Tumors-Derived Cell-Free Filtrates. *Annals of Hematology & Oncology*. 2022;9: 1-2022.
26. Scudamore CL, Busk N, Vowell K. A simplified necropsy technique for mice: making the most of unscheduled deaths. *Lab Anim*. 2014;48(4): 342-4.
27. Nikitin AY, Alcaraz A, Anver MR, Bronson RT, Cardiff RD, Dixon D, Fraire AE, Gabrielson EW, Gunning WT, Haines DC, Kaufman MH, Linnoila RI, Maronpot RR, Rabson AS, Reddick RL, Rehm S, Rozengurt N, Schuller HM, Shmidt EN, Travis WD, Ward JM, Jacks T. Classification of proliferative pulmonary lesions of the mouse: recommendations of the mouse models of human cancers consortium. *Cancer Res*. 2004;64(7): 2307-16.
28. NTP. Nonneoplastic Lesion Atlas. 2023 [cited 2023; National Toxicology Program]. Available from: https://ntp.niehs.nih.gov/atlas/nnl/respiratory-system/lung
29. Arnold M, Singh D, Laversanne M, Vignat J, Vaccarella S, Meheus F, Cust AE, de Vries E, Whiteman DC, Bray F. Global Burden of Cutaneous Melanoma in 2020 and Projections to 2040. *JAMA Dermatol*. 2022;158(5): 495-503.

30. Schroder R, Illert AL, Erbes T, Flotho C, Lubbert M, Duque-Afonso J. The epigenetics of breast cancer - Opportunities for diagnostics, risk stratification and therapy. *Epigenetics*. 2022;17(6): 612-24.
31. Siegel RL, Miller KD, Fuchs HE, Jemal A. Cancer statistics, 2022. *CA Cancer J Clin*. 2022;72(1): 7-33.
32. Yeo D, Giardina C, Saxena P, Rasko JEJ. The next wave of cellular immunotherapies in pancreatic cancer. *Mol Ther Oncolytics*. 2022;24: 561-76.
33. Alekseenko I, Kondratyeva L, Chernov I, Sverdlov E. From the Catastrophic Objective Irreproducibility of Cancer Research and Unavoidable Failures of Molecular Targeted Therapies to the Sparkling Hope of Supramolecular Targeted Strategies. *Int J Mol Sci*. 2023;24(3).
34. Yang N, Xiao W, Song X, Wang W, Dong X. Recent Advances in Tumor Microenvironment Hydrogen Peroxide-Responsive Materials for Cancer Photodynamic Therapy. *Nanomicro Lett*. 2020;12(1): 15.
35. Berraondo P, Sanmamed MF, Ochoa MC, Etxeberria I, Aznar MA, Perez-Gracia JL, Rodriguez-Ruiz ME, Ponz-Sarvise M, Castanon E, Melero I. Cytokines in clinical cancer immunotherapy. *Br J Cancer*. 2019;120(1): 6-15.
36. Costa-Machado LF, Fernandez-Marcos PJ. The sirtuin family in cancer. *Cell Cycle*. 2019;18(18): 2164-96.
37. Propper DJ, Balkwill FR. Harnessing cytokines and chemokines for cancer therapy. *Nat Rev Clin Oncol*. 2022;19(4): 237-53.
38. Wen Y, Zhu Y, Zhang C, Yang X, Gao Y, Li M, Yang H, Liu T, Tang H. Chronic inflammation, cancer development and immunotherapy. *Front Pharmacol*. 2022;13: 1040163.
39. Gloriane CLH, Severino Imasa M, Juat N, Hernandez KV, May Sayo T, Cristal-Luna G, Marie Asur-Galang S, Bellengan M, John Duga K, Brian Buenaobra B, De Los Santos MI, Medina D, Samo J, Minerva Literal V, Andrew Bascos N, Sy-Naval S. Expression landscapes in non-small cell lung cancer shaped by the thyroid transcription factor 1. *Lung Cancer*. 2023;176: 121-31.
40. Wang X, Langer EM, Daniel CJ, Janghorban M, Wu V, Wang XJ, Sears RC. Altering MYC phosphorylation in the epidermis increases the stem cell population and contributes to the development, progression, and metastasis of squamous cell carcinoma. *Oncogenesis*. 2020;9(9): 79.
41. Yuan X, Xu D. Telomerase Reverse Transcriptase (TERT) in Action: Cross-Talking with Epigenetics. *Int J Mol Sci*. 2019;20(13).
42. Hamad SH, Montgomery SA, Simon JM, Bowman BM, Spainhower KB, Murphy RM, Knudsen ES, Fenton SE, Randell SH, Holt JR, Hayes DN, Witkiewicz AK, Oliver TG, Major MB, Weissman BE. TP53, CDKN2A/P16, and NFE2L2/NRF2 regulate the incidence of pure- and combined-small cell lung cancer in mice. *Oncogene*. 2022;41(25): 3423-32.
43. Janker F, Weder W, Jang JH, Jungraithmayr W. Preclinical, non-genetic models of lung adenocarcinoma: a comparative survey. *Oncotarget*. 2018;9(55): 30527-38.
44. Hu Z, Curtis C. Looking backward in time to define the chronology of metastasis. *Nat Commun*. 2020;11(1): 3213.
45. Riggio AI, Varley KE, Welm AL. The lingering mysteries of metastatic recurrence in breast cancer. *Br J Cancer*. 2021;124(1): 13-26.
46. Compton C. Cancer Initiation, Promotion, and Progression and the Acquisition of Key Behavioral Traits. 2020. p. 25-48.